D6-19770
November 1967

Crack Extension in Several High-Strength Steels Loaded in 3.5% Sodium Chloride Solution

C. S. Carter

The BOEING Company
Commercial Airplane Division
Renton, Washington

Sponsored by
Advanced Research Projects Agency
ARPA Order No. 878

Crack Extension in Several High-Strength Steels Loaded in 3.5% Sodium Chloride Solution

C. S. Carter

Abstract

The morphology of crack growth was determined on precracked, notched bend specimens of 300M, H11, Maraging 250, 4330V, 9Ni-4Co-0.30C, and 9Ni-4Co-0.45C (martensitic and bainitic) steels four-point loaded in 3.5% sodium chloride solution. Crack extension from the tip of the fatigue precrack was either by a single crack that propagated along the fatigue crack plane (Type 1 cracking) or by two divergent cracks that propagated at an angle to the fatigue crack plane (Type 2 cracking). The 4330V, 9Ni-4Co-0.30C, and 9Ni-4Co-0.45C (bainitic) showed either Type 1 or Type 2 cracking, depending on the initial stress-intensity level K_{Ii}. The remaining steels exhibited only Type 1 cracking. The state of stress had a significant effect on the morphology of Type 2 cracks. The morphology suggests that Type 2 cracking is a result of environmental cracking along crack-tip plastic zones. The influence of yield strength on K_{ISCC} can be described by an empirical expression.

The author is associated with the Commercial Airplane Division of The Boeing Company, Renton, Washington. This research was supported by the Advanced Research Projects Agency of the Department of Defense (ARPA Order No. 878) and was monitored by the Naval Research Laboratory under Contract No. N00014-66-C0365.

Introduction

Catastrophic brittle fracture will occur in a load-bearing, high-strength steel component when a crack of critical size is present. The critical size is determined by the stress level and the fracture toughness of the steel. A crack of subcritical size can extend to critical size during sustained loading in a variety of environments, provided that the crack-tip stress intensity is greater than the threshold value K_{ISCC} (1,2). Since crack growth has been attributed to hydrogen embrittlement, stress corrosion, or a combination of both, to avoid specifying a mechanism, the term "environmental cracking" will be used in this report.

The aims of this study were to determine, using fatigue precracked specimens:

- The morphology of environmental cracking in several high-strength steels in 3.5% sodium chloride solution
- The factors influencing crack morphology
- The effect of crack morphology on the initiation of brittle fracture

Previous work on crack morphology in aqueous environments has been handicapped by the use of plain, unnotched specimens in which surface pitting preceded crack initiation (3,4,5). The random and multiple formation of pits and pit-cracks, with stress field interaction of neighbors, made interpretation of morphology difficult. The introduction of a fatigue precrack removes the need for pit formation and allows a fracture mechanics analysis of crack extension (1,6).

Materials and Testing

The resistance of several high-strength steels to environmental cracking in 3.5% sodium chloride solution was recently determined by The Boeing Company as part of a study for the Federal Aviation Agency (7). Fatigue precracked specimens were employed, and the fractured specimens were used for the present investigation. A brief discussion of the testing techniques used in the FAA study, together with some of the experimental results, follows.

Test Material

Three billets were obtained of each of the following consumable-electrode vacuum-melted high-strength steels:

1. 4330V
2. 9Ni-4Co-030C
3. H11
4. 9Ni-4Co-0.45C (martensitic and bainitic conditions)
5. 300M
6. Maraging (18% Ni) 250

The first three alloys were heat treated to ultimate tensile strengths in the range 220 to 240 ksi, whereas the others were heat treated to strengths above 250 ksi. Details of the chemical composition, heat treatment, mechanical properties, and plane strain fracture toughness have been reported previously (7).

Precracked Fatigue Specimens

At least three single-edge cracked specimens (Fig. 1) were machined in the transverse grain direction from each billet.

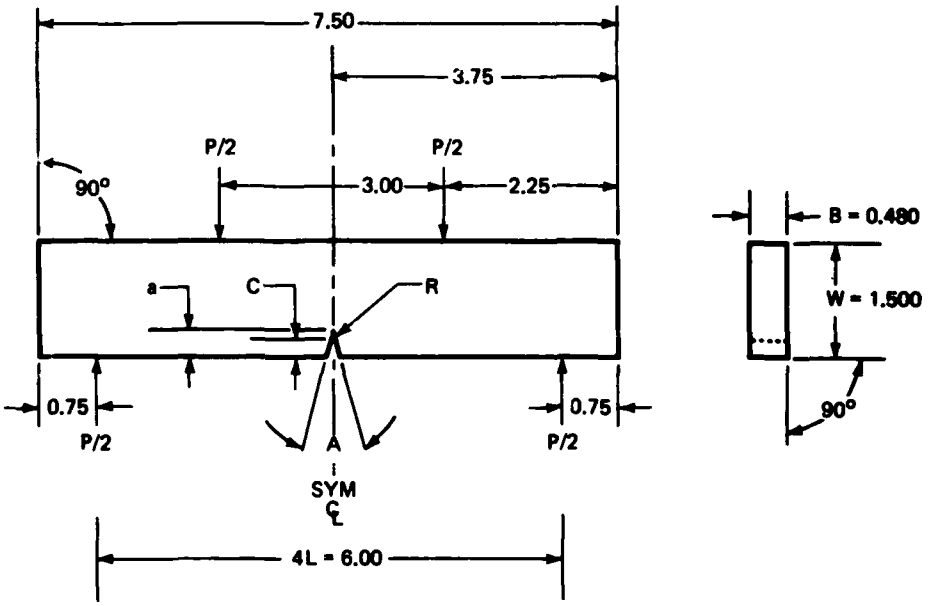

A = 45° NOTCH ANGLE
R = 0.011 MAX NOTCH RADIUS
C = 0.225 ± 0.001 NOTCH DEPTH
a = NOTCH DEPTH PLUS AVERAGE FATIGUE CRACK DEPTH
B = 0.480 ± 0.001–SPECIMEN WIDTH
W = 1.500 ± 0.001–SPECIMEN DEPTH
L = 1.50 MOMENT ARM

ALL DIMENSIONS IN INCHES

Fig. 1 Notched bend specimen

Environmental Testing

The specimens were placed in a Teflon-coated chamber and four-point loaded in bending to the desired initial stress-intensity level K_{Ii}. This was given by the expression (8):

$$K = \frac{PL}{BW^{3/2}} \left\{ \left(\frac{1}{1-\mu^2} \right) \left[34.7\left(\frac{a}{W}\right) - 55.2\left(\frac{a}{W}\right)^2 + 196\left(\frac{a}{W}\right)^3 \right] \right\}^{1/2} \quad (1)$$

where: P = applied load
L = moment arm
B = thickness
W = width
μ = Poisson's ratio
a = notch depth + fatigue crack depth

The chamber was then filled with 3.5% sodium chloride solution so that the specimen was submerged to a depth of 1 to 1.4 in. The initial applied load was maintained until failure occurred or until 10,000 min had elapsed. Specimens removed from the sodium chloride solution prior to failure were subsequently fractured in air and examined for crack growth.

During the tests, a variation of from 5 to 7 pH, due to variations in the pH of the distilled water used to prepare the sodium chloride solution, was detected. However, recent work by Van Der Sluys (9) suggests that this does not significantly affect the results.

Results of Bend Tests

The results of the tests were plotted as curves of K_{Ii}/K_{IC} versus time to failure where K_{IC} was the average plane strain fracture toughness for each steel (Fig. 2). Estimates were made of the threshold stress-intensity level K_{ISCC} below which environmental cracking does not occur under plane strain conditions (Table 1). Threshold levels were not clearly established for 9Ni-4Co-0.30C and Maraging 250, since all the specimens of these alloys displayed some crack growth. However, the estimated value for the Maraging 250 steel showed good agreement with values reported by other investigators for this material (10). The curves of K_{Ii}/K_{IC}, Fig. 2, suggest that there is an incubation period prior to environmental crack initiation and are similar to the curves reported by other investigators (1,2,11-15).

Estimation of $K_{I\delta}$

The bend tests were conducted at constant load. Consequently, as the environmental crack extended through the specimen, the stress intensity at the crack tip (K_I) increased from the initial K_{Ii} level to a critical value at which rapid brittle fracture occurred (Fig. 3). This critical stress intensity has been designated $K_{I\delta}$. Since K_{IC} is the critical stress intensity for brittle fracture from a sharp precrack, the ratio $K_{I\delta}/K_{IC}$ provides a measure of the blunting at

the crack tip. A $K_{I\delta}/K_{IC}$ value of 1.0 indicates an absence of blunting, whereas higher ratios indicate environmental crack blunting by some mechanism.

Equation (1) is applicable only to specimens having an a/W value of less than 0.35. In many specimens the length of the environmental crack exceeded this limit. Therefore, to evaluate $K_{I\delta}$, a modified expression valid to crack length/width values of 0.60 was used (16):

$$K_{I\delta} = \frac{3PL\sqrt{a}\,(1-\mu^2)^{-1/2}}{BW^2}\left[1.99-2.47\left(\frac{a}{W}\right)+12.97\left(\frac{a}{W}\right)^2-23.17\left(\frac{a}{W}\right)^3+24.80\left(\frac{a}{W}\right)^4\right] \quad (2)$$

The notation is the same as for Eq. (1) except that the environmental crack length was included in a. The term $1-\mu^2$, not specified in Ref. 16, was included in Eq. (2) to be consistent with Eq. (1). $K_{I\delta}$ was not determined for specimens when the crack length exceeded 0.60 of the width of the specimen.

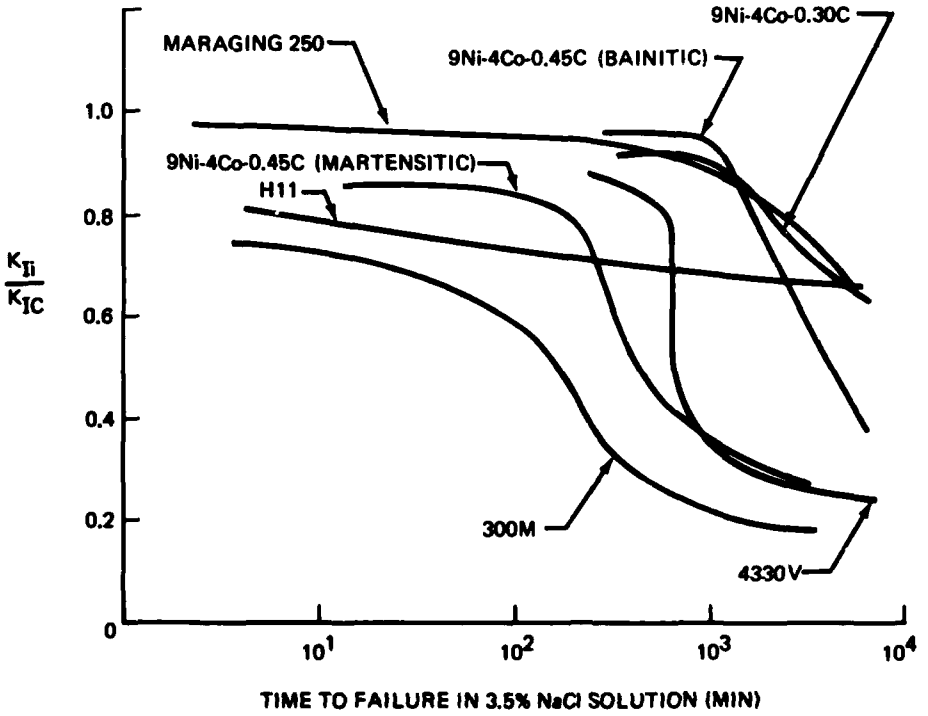

Fig. 2 Summary of sustained-loading characteristics (from Ref. 7)

Table 1 Estimated Threshold Stress-Intensity Levels in 3.5% Sodium Chloride Solution (from Ref. 7)

Alloy	Tensile Yield Strength* (ksi)	Ultimate Tensile Strength* (ksi)	Plane Strain Fracture Toughness,* K_{IC} (ksi $\sqrt{in.}$)	Estimated Threshold Level, K_{ISCC} (ksi $\sqrt{in.}$)
4330V	196	239	103	25
H11	188	219	54	30
9Ni-4Co-0.30C	200	231	116	45
300M	236	283	76	13
Maraging 250	249	259	92	45
9Ni-4Co-0.45C (martensitic)	236	276	69	15
9Ni-4Co-0.45C (bainitic)	220	266	89	20

* average

Crack Morphology

Two patterns of environmental crack extension were identified:

Type 1—a single symmetrical crack extending along the fatigue crack plane (Fig. 4A)

Type 2—two divergent cracks extending from the fatigue crack tip at an angle to the fatigue crack plane (Fig. 4B)

In both types of cracking, the crack planes were normal to the side surfaces of the specimen.

The 300M, H11, Maraging 250, and 9Ni-4Co-0.45C (martensitic) steels exhibited only Type 1 cracking. In the remaining steels both Type 1 and Type 2 cracking were observed. Because of this behavior, the crack morphology will be described as it pertains to the two groups of steels.

300M, H11, Maraging 250, and 9Ni-4Co-0.45C (Martensitic) Steels

In specimens of these four steels, the environmental crack generally extended symmetrically along the fatigue crack plane, that is, Type 1 cracking. Examination of the fracture surfaces revealed that in the Maraging 250 steel the crack had tunneled through the midsection of the specimen and shear lips had subsequently formed along

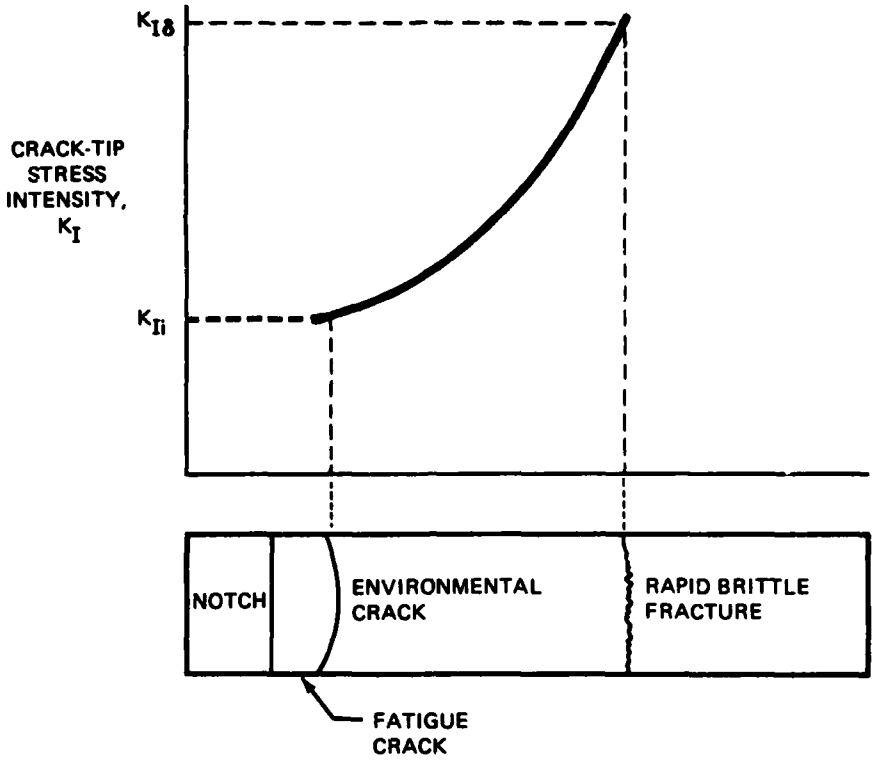

Fig. 3 Increase in stress intensity with increasing environmental crack length at constant load

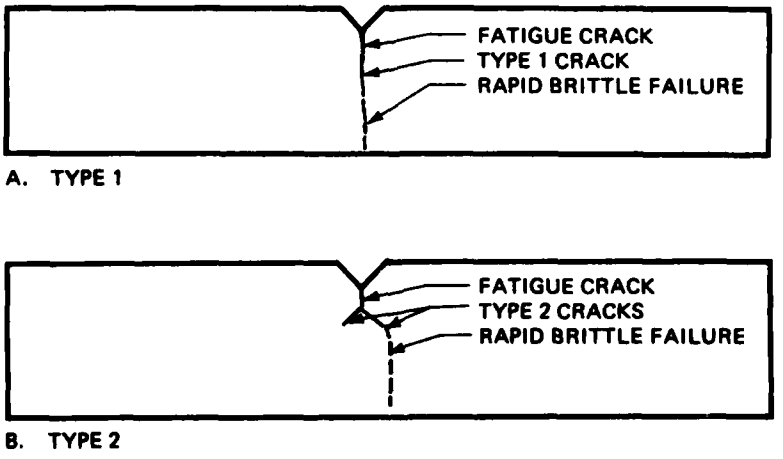

Fig. 4 Types of environmental crack extension

the side borders (Fig. 5). Tunneling and shear lips were absent from the fracture surface of 300M and 9Ni-4Co-0.45C (martensitic) (Figs. 6 and 7) and of H11 steel specimens. The differences observed among the steels in the degree of secondary cracking are discussed below.

300M. The secondary cracks in 300M steel specimens extended from the primary environmental crack during its growth through the specimen at an angle to the primary crack plane of about 20 deg. The secondary cracks become larger as the primary crack length, and hence K, increased (Fig. 8). These cracks did not extend through the specimen thickness, but apparently developed in random regions, so that a minimum stress intensity for secondary crack formation could not be confidently established.

The blunting effect associated with secondary cracks is shown by the $K_{I\delta}/K_{IC}$ values (Table 2), which in most specimens were significantly higher than unity. This was contrary to the results reported by Brown (2) on a 4340 steel for which $K_{I\delta}$ and K_{IC} were similar in magnitude; 300M and 4340 steels have similar chemical compositions except for a higher silicon content (1.6%) in 300M.

H11. Secondary cracks were absent in H11 steel. $K_{I\delta}$ values were not determined because of difficulty in visually discriminating between the environmental crack and the region of brittle fracture.

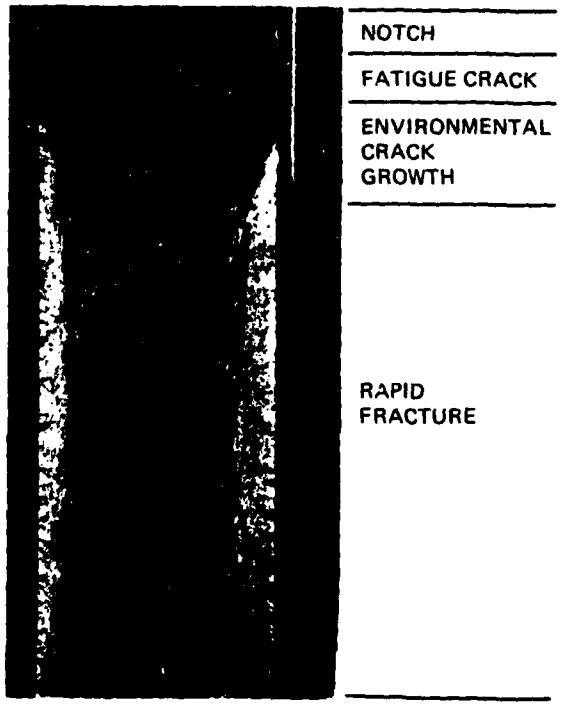

Fig. 5 Fracture surface of Maraging 250 (K_{Ii} = 79.2 ksi $\sqrt{in.}$)

Maraging 250. Secondary cracks were also absent in Maraging 250 steel. However, the $K_{I\delta}/K_{IC}$ values (Table 2) indicated that blunting had occurred to some extent in most specimens. This was attributed to tunneling by the environmental crack whereby the uncracked side borders restrained the initiation of rapid plane strain brittle fracture (Fig. 5).

9Ni-4Co-0.45C (Martensitic). The secondary cracks in 9Ni-4Co-0.45C (martensitic) steel extended at an angle of approximately 45 deg to the primary crack plane and were much longer than in 300M steel (Fig. 9). They had a morphology similar to that of Type 2 cracks, but extended from the primary Type 1 crack rather than from the fatigue precrack. The onset of secondary cracking appeared to require a minimum stress intensity at the crack tip; however, this varied from specimen to specimen within the range 40 to 60 ksi$\sqrt{in}$.

In most specimens, $K_{I\delta}$ was almost twice the magnitude of K_{IC} (Table 2), indicating the severe blunting effect associated with secondary cracks.

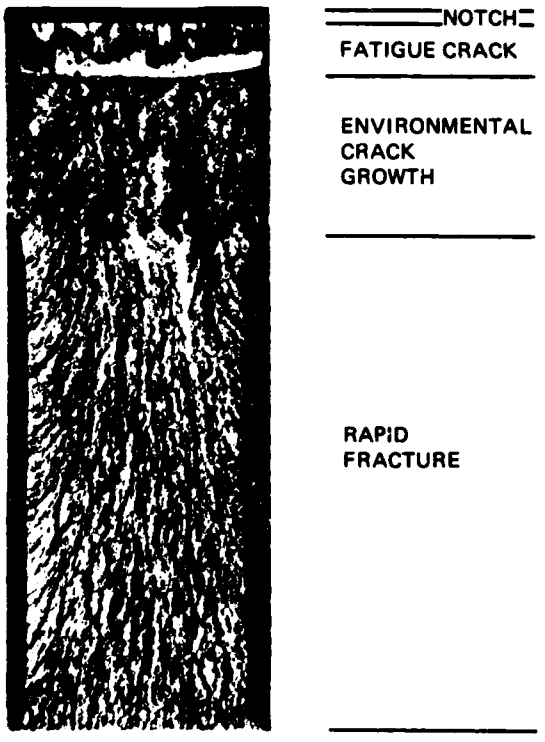

Fig. 6 Fracture surface of 300M (K_{Ii} = 64.4 ksi$\sqrt{in.}$)

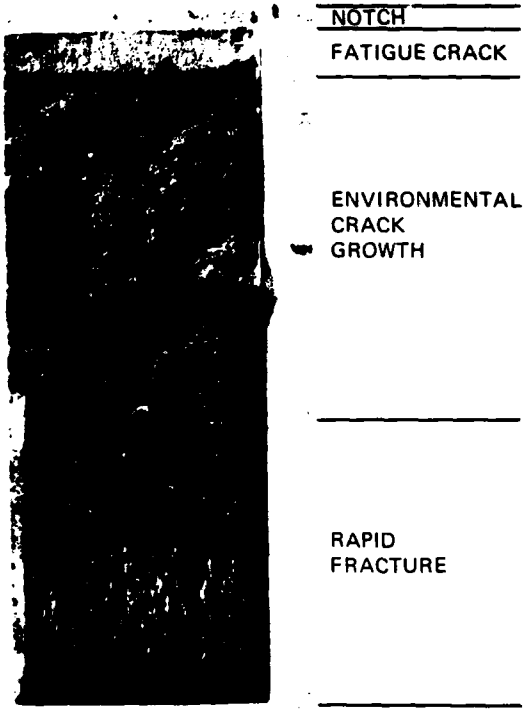

Fig. 7 Fracture surface of 9Ni-4Co-0.45C (martensitic) (K_{Ii} = 45.0 ksi $\sqrt{in.}$)

4330V, 9Ni-4Co-0.30C, and 9Ni-4Co-0.45C (Bainitic) Steels

These steels exhibited a transition from Type 1 to Type 2 cracking with testing at increasing K_{Ii} levels (Figs. 10 and 11). Type 1 cracks extended from the precrack with almost a complete absence of secondary crack development (Fig. 12) when K_{Ii} was less than a transition value. Above this value, Type 2 cracks formed (Figs. 13 to 15). The transition K_{Ii} value was different for each steel. However, when the transition is considered in relation to the ratio of K_{Ii}/Y, where Y is the tensile yield strength, similar values were obtained for each steel (Fig. 11).

The environmental cracks in these steels preferentially extended along the side surfaces and lagged at the midsection* (Figs. 16 to 18). This was particularly

*Brown and Srawley (16) have tentatively suggested that plane strain conditions are operative when $2.5\,(K/Y)^2$ is greater than the thickness. This requirement was maintained in most tests. However, plane stress relaxation must have occurred at the side surfaces, since plane strain conditions cannot be maintained at a free surface.

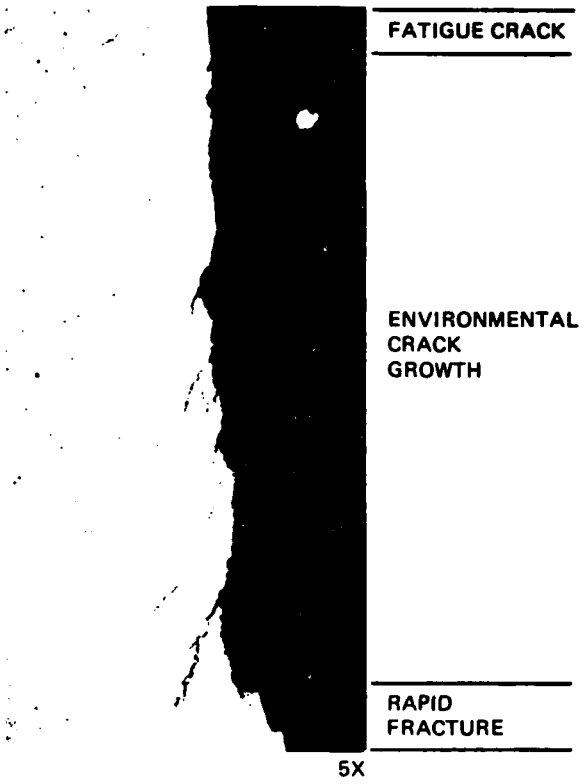

Fig. 8 Secondary cracks in 300M (K_{Ii} = 47.3 ksi$\sqrt{in.}$)

apparent in the 9Ni-4Co-0.45C (bainitic) specimens in which environmental cracks extended along the specimen sides, but were absent from the midsection in specimens loaded to K_{Ii} values close to K_{IC} (Fig. 18). This behavior is contrary to the current but unpublished theory which considers that plane stress regions are resistant to environmental cracking. In addition, the irregular shape of the cracks (Figs. 16 to 18) prevented the determination of any degree of blunting: Eq. (2) can only be applied to a straight crack front. The morphology of the Type 2 cracks at the side surface and at the midsection was significantly different. This was apparent in all three steels, and will be described, using the 4330V steel as a typical example.

At the side surface the cracks extended from the fatigue crack in the form of arcs (Figs. 13A, 14A, and 15A). Increasing K_{Ii}/Y had little influence on this morphology except that the arcs became rather more steeply inclined to the fatigue crack plane. At the midsection, however, the morphology was dependent on the ratio of K_{Ii} to Y. Close to the transition K_{Ii}/Y value, the morphology of cracks at the midsection was similar to that of cracks at the side surface (Figs. 13A and 13B).

At higher K_{Ii}/Y levels, both divergent cracks extended along planes that were inclined to the fatigue crack plane at an angle within the range 45 to 75 deg (Figs. 14B and 15B). In one specimen, the angle was 90 deg (Fig. 19). Also, pairs of cracks parallel to the fatigue crack plane initiated within the first formed pairs at high K_{Ii}/Y ratios (Figs. 14B and 15B).

Table 2 Comparative $K_{I\delta}$ and K_{IC} Values

Alloy	Heat Number	Yield Strength (ksi)	Plane Strain Fracture Toughness, K_{IC} (ksi$\sqrt{in.}$)	Initial Stress Intensity, K_{Ii} (ksi$\sqrt{in.}$)	Critical Stress Intensity, $K_{I\delta}$ (ksi$\sqrt{in.}$)	$K_{I\delta}/K_{IC}$
300M	3931531P	233	78.9	64.4	104	1.32
				54.1	126	1.60
				47.3	148	1.88
				40.1	101	1.28
				29.2	104	1.38
	3951531R	239	81.6	47.5	147	1.80
				38.8	130	1.60
				28.2	102	1.25
	09715	236	67.4	47.3	106	1.57
				39.6	91.5	1.36
				33.8	113	1.67
				27.8	92.5	1.37
				20.8	71.5	1.06
				20.2	71.5	1.06
9Ni-4Co-0.45C (martensitic)	3931141	237	76.4	62.1	144	1.89
				61.1	134	1.76
				57.3	173	2.26
				45.0	113	1.48
	3931120	233	66.0	55.7	91	1.37
				51.5	152	2.30
				45.0	128	1.94
	3882720	237	58.8	47.0	109	1.64
				40.4	92	1.38

(continued)

Table 2 Comparative $K_{I\delta}$ and K_{IC} Values (Continued)

Alloy	Heat Number	Yield Strength (ksi)	Plane Strain Fracture Toughness, K_{IC} (ksi$\sqrt{in.}$)	Initial Stress Intensity, K_{Ii} (ksi$\sqrt{in.}$)	Critical Stress Intensity, $K_{I\delta}$ (ksi$\sqrt{in.}$)	$K_{I\delta}/K_{IC}$
Maraging 250	24676	262	88.0	83.5	119	1.35
				79.2	113	1.28
				69.1	110	1.25
				61.6	91.3	1.04
				82.5	86.6	0.99
	09148	240	90.0	81.6	104	1.14
				75.6	107	1.18
				53.3	94.5	1.04
	3930879	241	98.9	94.4	125	1.26
				89.9	113	1.14

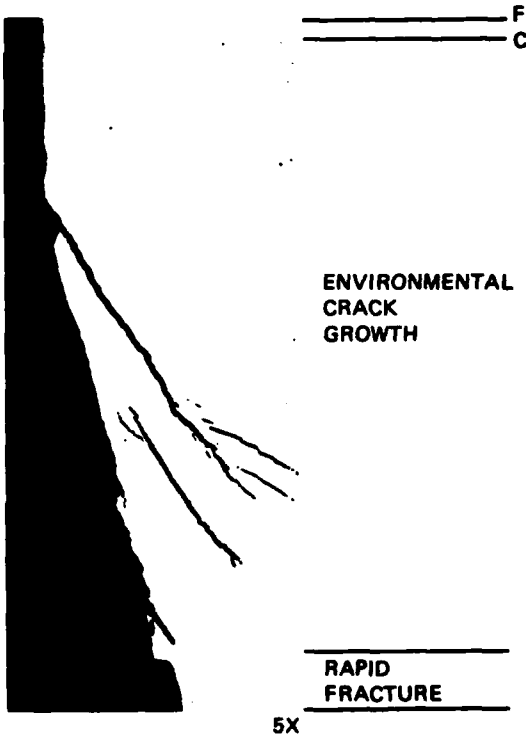

Fig. 9 Secondary cracks in 9Ni-4Co-0.45C (martensitic) (K_{Ii} = 33.8 ksi $\sqrt{in.}$)

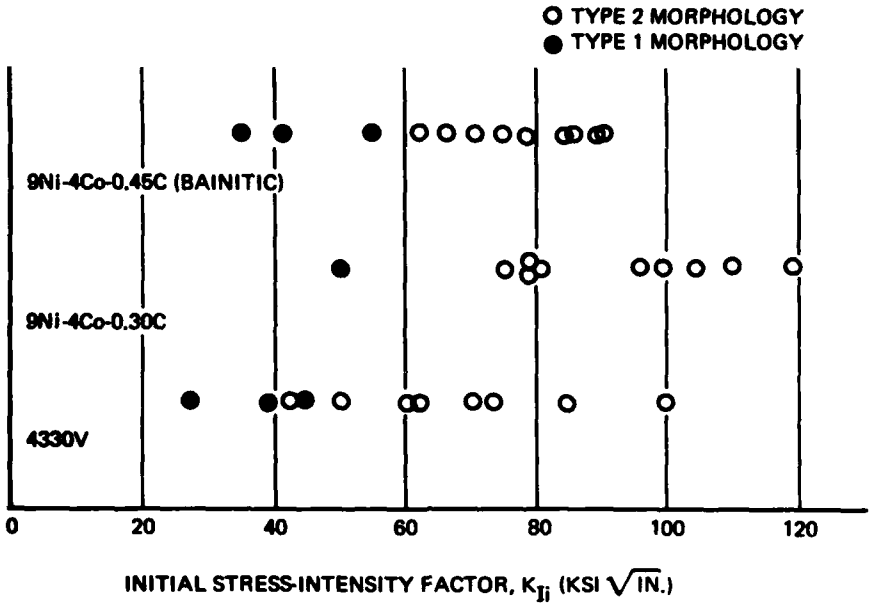

Fig. 10 Influence of K_{Ii} on crack morphology

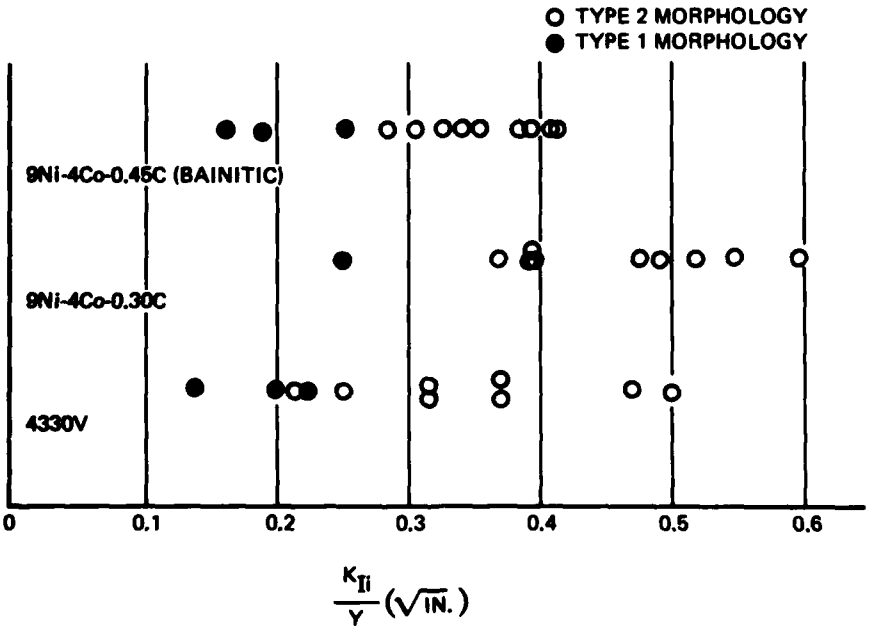

Fig. 11 Influence of K_{Ii}/Y on crack morphology

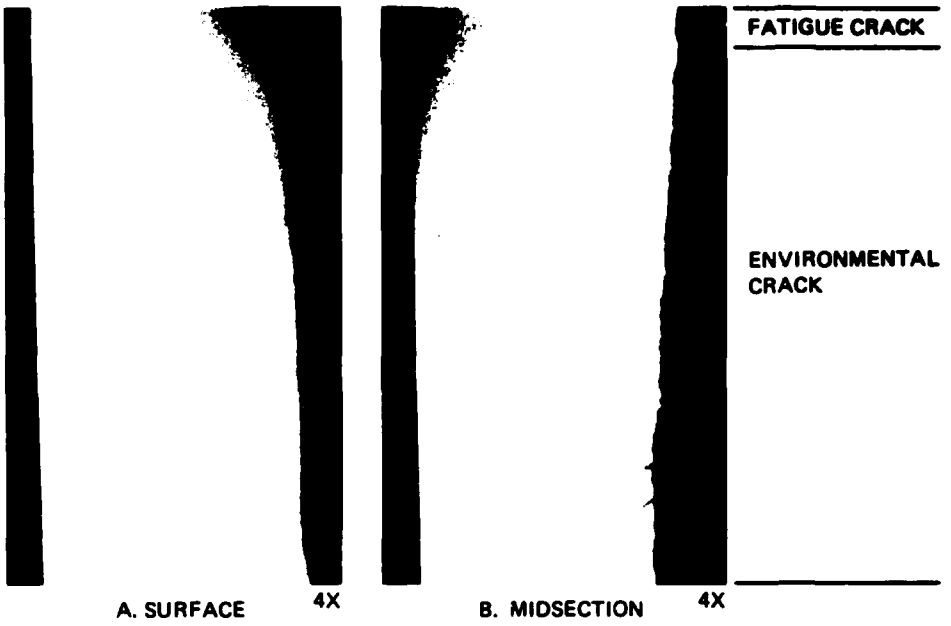

Fig. 12 Section of failed 4330V notched bend specimen (K_{Ii} = 34.2 ksi $\sqrt{in.}$)

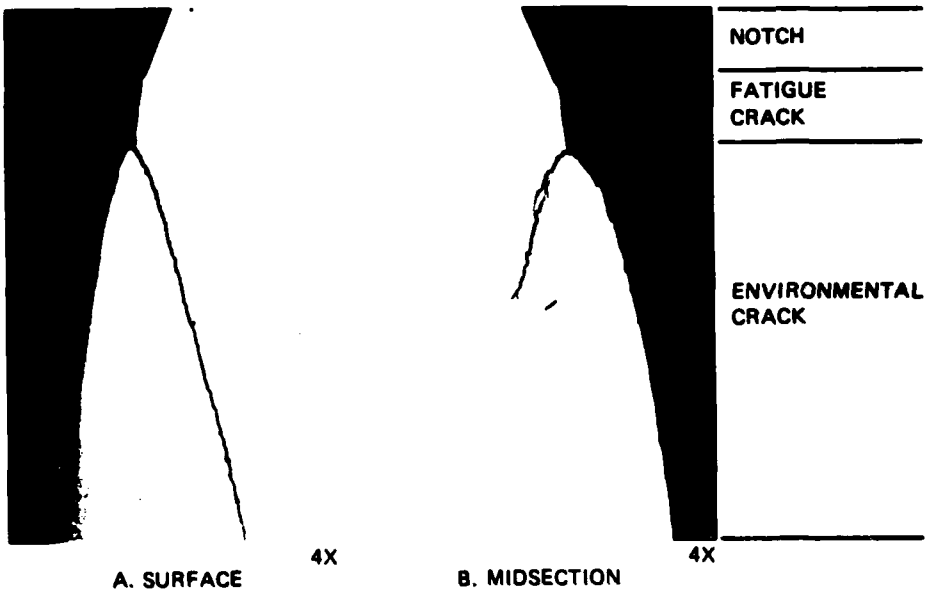

Fig. 13 Section of failed 4330V notched bend specimen (K_{Ii} = 62.2 ksi $\sqrt{in.}$)

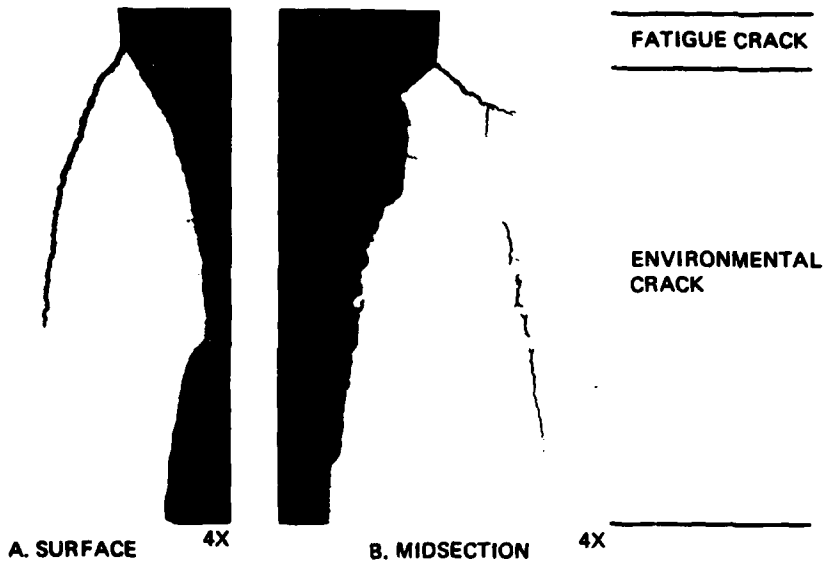

Fig. 14 Section of failed 4330V notched bend specimen (K_{Ii} = 73.4 ksi $\sqrt{in.}$)

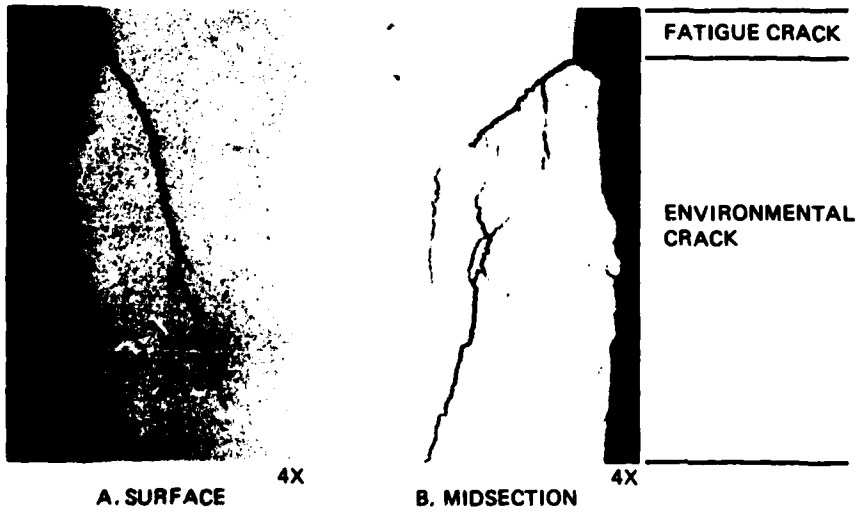

Fig. 15 Section of failed 4330V notched bend specimen (K_{Ii} = 83.9 ksi $\sqrt{in.}$)

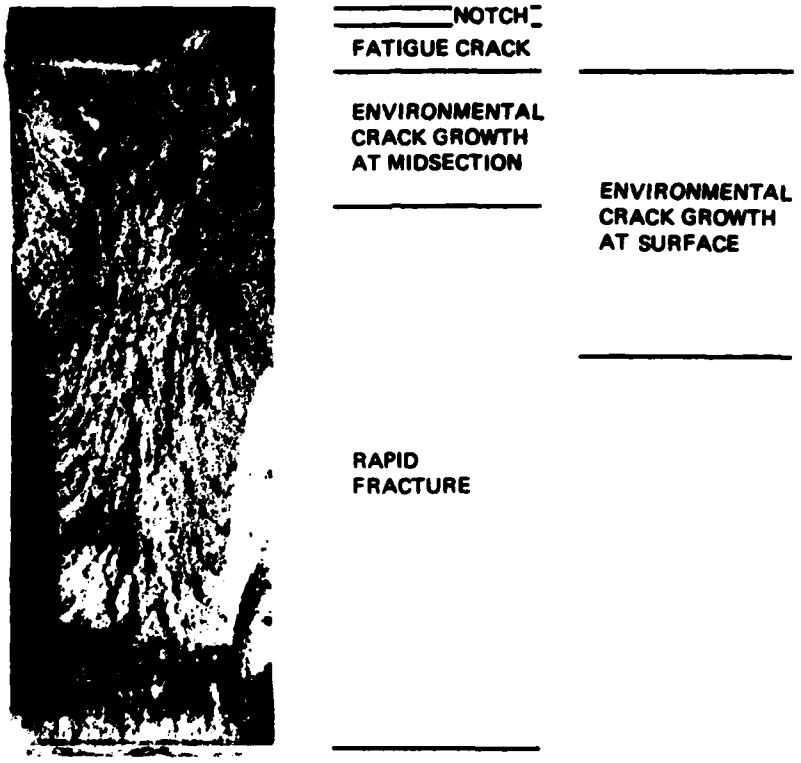

Fig. 16 Fracture surface of 4330V (K_{Ii} = 62.2 ksi$\sqrt{in.}$)

In several specimens the Type 2 cracks had extended in certain areas by repeated formation of two divergent cracks, such as are visible in Figs. 13B, 14A, 15A, and 19. These cracks were analogous to the Type 2 cracks except that they were an order of magnitude smaller and initiated from the tip of the prior formed environmental crack.

Type 2 Cracking

Comparison of Plastic Yield Phenomena With Type 2 Crack Morphology

When a load is applied to a specimen containing a crack, plastic yielding occurs at the crack tip. The size and shape of this zone of plastic strain can be predicted theoretically by various methods (17). However, these methods are limited by the assumptions that must be made, particularly with regard to the strain-hardening

behavior of the material. Nevertheless, provided the plastic zone is very much smaller than the crack length, the zone size p can be estimated for plane strain conditions from (18):

$$p = \frac{1}{3\pi}\left(\frac{K_I}{Y}\right)^2 \qquad (3)$$

For plane stress conditions the zone is approximately three times larger.

The shape of the plastic zone has been experimentally delineated in a variety of materials by several workers (17, 19-23), who demonstrated the influence of state of stress (19,22) and strain-hardening characteristics (23). Under plane stress conditions, the plastic zones nucleate from the crack tip as two divergent arcs that extend, under rising load, across the reduced section below the notch. With decreasing strain-hardening resistance of the material the zones become narrower (23). Under plane strain conditions, it has been demonstrated by Hahn (19) that two plastic zones diverge along straight paths, each inclined at an angle of approximately 75 deg to the crack plane. These observations are similar to Type 2 crack morphology in both plane stress and plane strain regions.

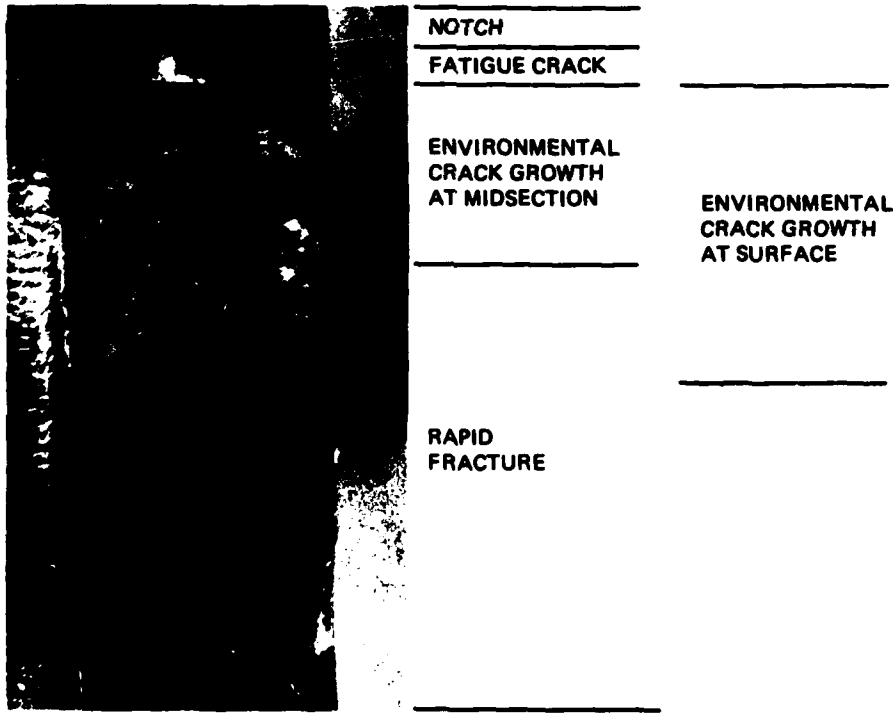

Fig. 17 Fracture surface of 9Ni-4Co-0.30C (K_{Ii} = 119.2 ksi$\sqrt{in.}$)

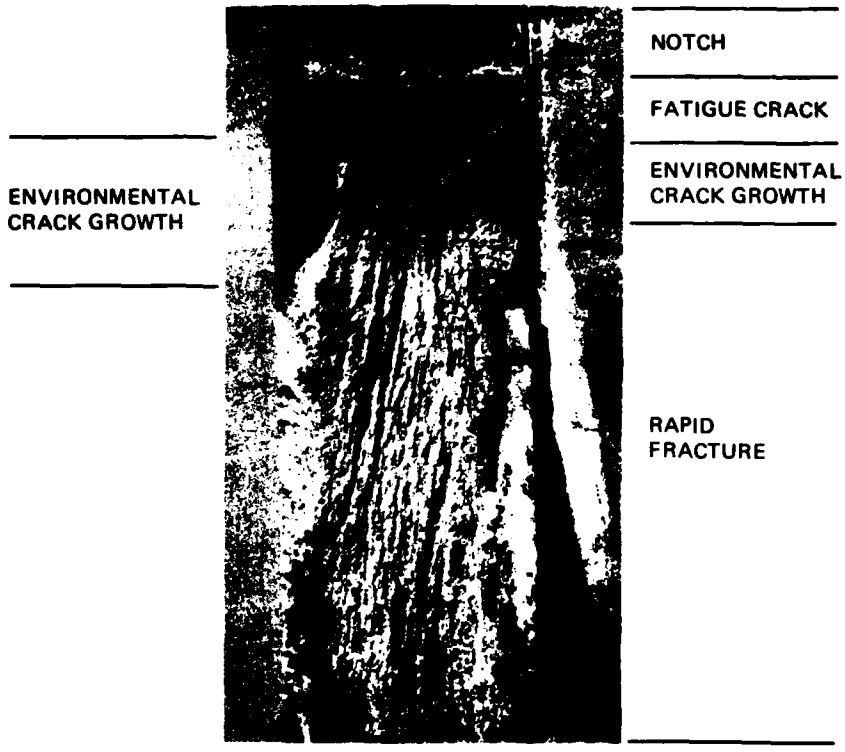

Fig. 18 Fracture surface of 9Ni-4Co-0.45C (bainitic) (K_{Ii} = 91.1 ksi $\sqrt{in.}$)

The size of the plastic zone that exists ahead of the fatigue precrack prior to crack extension has been determined to be an order of magnitude smaller than the total extent of environmental cracking. For example, Eq. (3) indicates that, under plane strain conditions, a crack at a typical K_{Ii} level of 85 ksi$\sqrt{in.}$ in a material of 200-ksi yield strength would have a plastic zone 0.02 in. long at the tip. The divergent cracks within the main Type 2 cracks (Figs. 13B, 14A, 15A, and 19) were of this order of size, and their morphology was similar to that described. This suggests that the cracks extended along the plastic zones which formed ahead of the growing environmental cracks. Truman et al. (24) have directly observed the operation of this mechanism in martensitic stainless steels.

An interesting example of Type 2 cracking is illustrated in Fig. 19, which shows the crack at midsection in a 4330V specimen loaded to a K_{Ii}/Y value of 0.50. The morphology of the initial crack extension ahead of the fatigue precrack, that is, of the three cracks at 90 deg to each other, is identical to that of the plastic zone shown by Hahn (Fig. 4c in Ref. 19) for a silicon-iron specimen loaded to a K_I/Y of 0.45.

Fig. 19 Unfailed 4330V notched bend specimen (K_{Ii} = 99.0 ksi$\sqrt{in.}$)

It would be expected that the morphology of a crack extending at constant load by repeated propagation along the crack-tip plastic zone would be similar to that of a plastic zone spreading under rising load not involving cracking. It is therefore considered that the Type 2 cracks initially extend along the plastic zone at the fatigue crack tip. Subsequent growth requires continuous repetition of this process ahead of the extending environmental crack and the morphology of Type 2 cracks is a result of this mode of crack extension. The dependence of the transition from Type 1 to Type 2 cracking on the ratio of K_{Ii} to Y suggests that a minimum-size plastic zone may be required to promote Type 2 cracks. Since the strain-hardening exponent influences the shape of the plastic zone as well as the magnitude and distribution of the plastic strain, this parameter may have a significant influence on the crack morphology.

Mechanisms

Beacham et al. (25) observed Type 2 cracks in Maraging 200 steel, and attributed them to preferential cracking through bands of segregation lying normal to the fatigue crack plane. However, the Type 2 cracks discussed in this report could not be related to minor segregation bands that were present. Furthermore, their mechanism cannot explain the influence of state of stress and K_{Ii} level on crack morphology.

Type 2 cracks are inconsistent with the Troiano model (26) of hydrogen embrittlement, which predicts Type 1 cracking. Nevertheless, a hydrogen embrittlement mechanism cannot be dismissed, since there are other models of hydrogen embrittlement (27, 28), and Boniszewski et al. (29) have observed Type 2 cracking in hydrogen-charged notched tension specimens. Alternatively, the crack-tip plastic zones may be anodic to the surrounding elastically strained material and thus provide an active path for stress-corrosion cracking. In fact, Scully and Hoar (30) have observed Type 2 stress-corrosion cracks in notched bend specimens of 18-8 austenitic stainless steel exposed to boiling 42% aqueous magnesium chloride solution. It appears, therefore, that Type 2 cracks cannot be identified with a specific mechanism. It is intended to conduct electrochemical polarization studies in an attempt to establish the mechanism.

Type 1 Cracking

The fractographic examinations that had been conducted previously on the failed specimens (7) showed intergranular fracture in the region of environmental cracking in all the specimens except the Maraging 250 steel, which exhibited transgranular failure. Other investigators have reported similar observations (4), except that both intergranular and transgranular cracking have been reported in *different heats of maraging steel* (31).

Fractographic examination revealed, in certain specimens that exhibited Type 1 cracking, a band of dimpled fracture (that is, microvoid coalescence) between the fatigue crack tip and the intergranular crack. Other specimens in the same material showed intergranular cracks directly below the fatigue crack tip. Therefore, under certain conditions, environmental cracks must have initiated a distance ahead of the fatigue crack tip, the intermediate zone subsequently breaking by ductile rupture.

To establish the position of crack initiation with respect to the plastic zone boundary, the following investigation was conducted. The length of the dimpled fracture band ahead of the fatigue crack tip was measured by fractography on several specimens. The length of the plastic zone at the fatigue crack tip was estimated from Eq. (3). The results may be compared in Fig. 20 as a function of K_{Ii}/Y. When K_{Ii}/Y was less than approximately 0.2, intergranular cracking initiated at the fatigue crack tip. At higher K_{Ii}/Y values, intergranular cracking initiated within the plastic zone.

When plane strain conditions are operative at a crack tip, the plastic zone is constrained by the surrounding elastic material and the triaxial stress system can sustain high tensile stresses normal to the crack plane. The magnitude of the maximum normal stress σ_{max}, which depends on a number of factors, can approach three times the uniaxial yield stress (32,33). If it is assumed that environmental crack initiation requires a critical normal stress to be reached ahead of the pre-

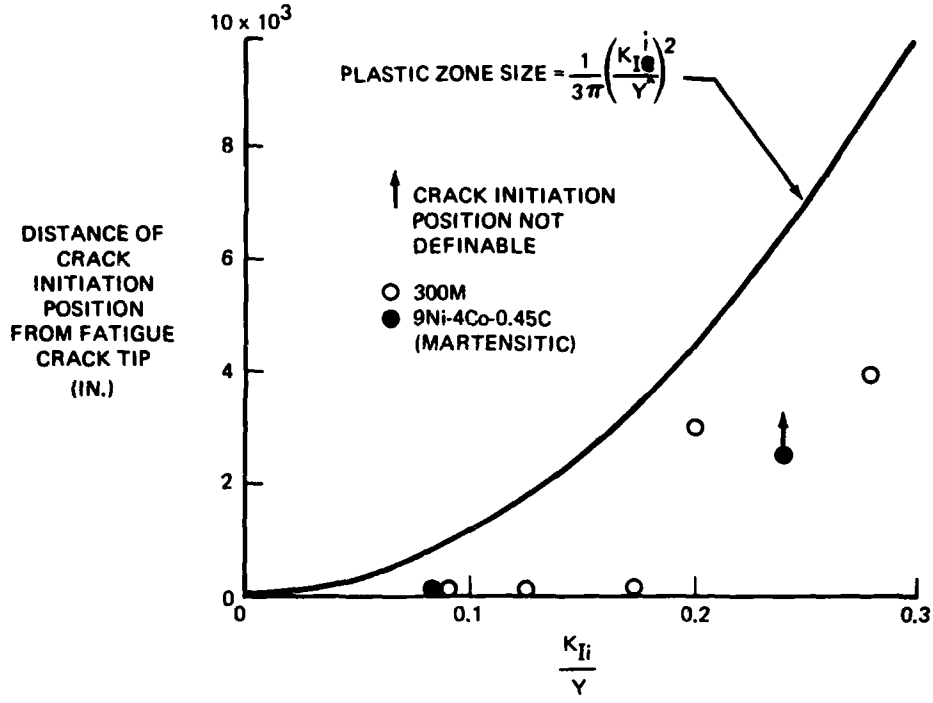

Fig. 20 Comparison of crack initiation position with plastic zone size

crack (34), the threshold stress-intensity level K_{ISCC} should be directly related to this critical stress. Hahn and Rosenfield (35) have recently suggested that the stress intensity K and the yield stress Y can be related to σ_{max}, for plane strain conditions, by:

$$\sigma_{max} = \left[1 + 2\ \frac{K}{Y}\right] Y \qquad (4)$$

Equation (4) was derived empirically from results obtained on mild steel, and the basic assumptions have been criticized by Tetleman (36). Under these circumstances, application of Eq. (4) to high-strength steels was certainly speculative. Nevertheless, the K_{ISCC} and yield strength values (Table 1) have been used in Eq. (4) to estimate a critical normal stress for crack initiation, that is, the σ_{max} value corresponding to K_{ISCC}. The estimates are shown in Table 3. Similar critical stress values within the range 246 to 266 ksi were exhibited by 4330V, H11, 300M, and 9Ni-4Co-0.45C (martensitic and bainitic) steels. Maraging 250 had the highest critical stress, 340 ksi, and 9Ni-4Co-0.30C had an intermediate value, 290 ksi. The latter value should be treated with caution in light of the uncertainty of the K_{ISCC} value of this steel.

Table 3 Estimates of Critical Stress for Crack Initiation

Alloy	Critical Normal Stress (ksi)
4330V	246
H11	246
9Ni-4Co-0.45C (bainitic)	260
300M	262
9Ni-4Co-0.45C (martensitic)	266
9Ni-4Co-0.30C	290
Maraging 250	339

Sandoz (10) has recently published a summary plot of K_{ISCC} data as a function of tensile yield strength. The relationship predicted with Eq. (4) has been superimposed on this plot (Fig. 21) for two selected values of the critical normal stress, 250 ksi for the low-alloy and 9Ni-4Co-0.45C steels and 340 ksi for the 18% Ni maraging steels. The two lines show a reasonable fit to their respective data points over a range of yield strengths.

When plane stress conditions exist, plastic constraint cannot develop and the maximum stress at the crack tip has been given as (37):

$$\sigma_{max} = 1.15\ Y \qquad (5)$$

For critical stress values similar in magnitude to the yield strength, crack initiation can occur under both plane stress and plane strain conditions. Equation (4) indicates that this will occur when K_{ISCC}/Y is less than approximately 0.1. Under these conditions, decreasing thickness would not be expected to influence the threshold stress intensity. If the critical stress is significantly greater than the yield stress, the environmental crack resistance of the plane stress regions will depend on their ability to strain harden to the critical stress.

The appearance of the fractured specimens lends some credence to this model. Shear lips were absent from the regions of environmental cracking in 300M and 9Ni-4Co-0.45C (martensitic) steels (Figs. 6 and 7), indicating that

the plane stress regions were susceptible to environmental cracking. These steels had K_{ISCC}/Y values less than 0.1. The calculated critical stress of 340 ksi for the Maraging 250 steel was much greater than the yield stress, and the strain-hardening exponent of this steel is small. The shear lips present in the region of environmental cracking (Fig. 5) in Maraging 250 steel are therefore predicted by the model. Ductile failure of these plane stress regions, which requires a critical strain, occurred before the critical stress for environmental cracking was achieved.

There is a signigicant difference between the microstructure of the low-alloy steels, which had the lowest critical stresses, and the Maraging 250 steel, which had the highest critical stress. It has been shown that the microstructures of the low-alloy (38) and the 9Ni-4Co-0.45C (martensitic) (39) steels contain martensite plates that are internally twinned, whereas transformation twins are absent from Maraging 250 steel (40). Hence, transformation twinning appears to have a detrimental influence on environmental cracking resistance. It is also relevant to note that the recently developed 10Ni-Co-Cr-Mo steels, which have excellent stress-corrosion resistance, have an untwinned martensitic structure (41). Boniszewski et al. (29) have observed a similar effect of transformation twinning on resistance to hydrogen embrittlement.

Practical Implications

Laminated Structures

Attention has recently been given to multiple bonding of thin sheets of high-strength steels to form laminates (42). This technique promotes the development of plane stress conditions, with an attendant increase in fracture toughness. However, it has been suggested in this report that in steels with K_{ISCC}/Y values less than about 0.1 there is no improvement in K_{ISCC} level with decreasing thickness. Figure 21 indicates that for an ultimate tensile strength of 280 ksi, with commensurate tensile yield strengths of 240 and 275 ksi in low-alloy and maraging steels, the K_{ISCC}/Y value is less than 0.1 for all currently available steels. Under these circumstances, laminating would not improve resistance to environmental cracking.

Beneficial Effects of Crack Blunting

The conditions for brittle fracture are given by (6):

$$a = \left[\frac{K_{Ic}}{\sigma}\right]^2 S \qquad (6)$$

where a is the critical crack length, σ is the applied stress, and S a geometrical factor that depends on crack shape and loading conditions. If the critical stress-intensity factor is increased from K_{IC} to $K_{I\delta}$, the critical length for failure

is increased by a factor of $(K_{I\delta}/K_{IC})^2$. All things being equal, the steels that exhibit extensive branch cracking will have a "blunting" advantage when used in circumstances where environmental cracking is a definite hazard.

Fracture mechanics is often used in service failure analysis. The stress level that caused failure is estimated from the size of the initial crack and the K_{IC} of the material. If branching has occurred and if K_{IC} rather than $K_{I\delta}$ is used, then the failure stress will be underestimated by a factor of $K_{I\delta}/K_{IC}$. For example, in 300M steel this would be a factor of about 1.5.

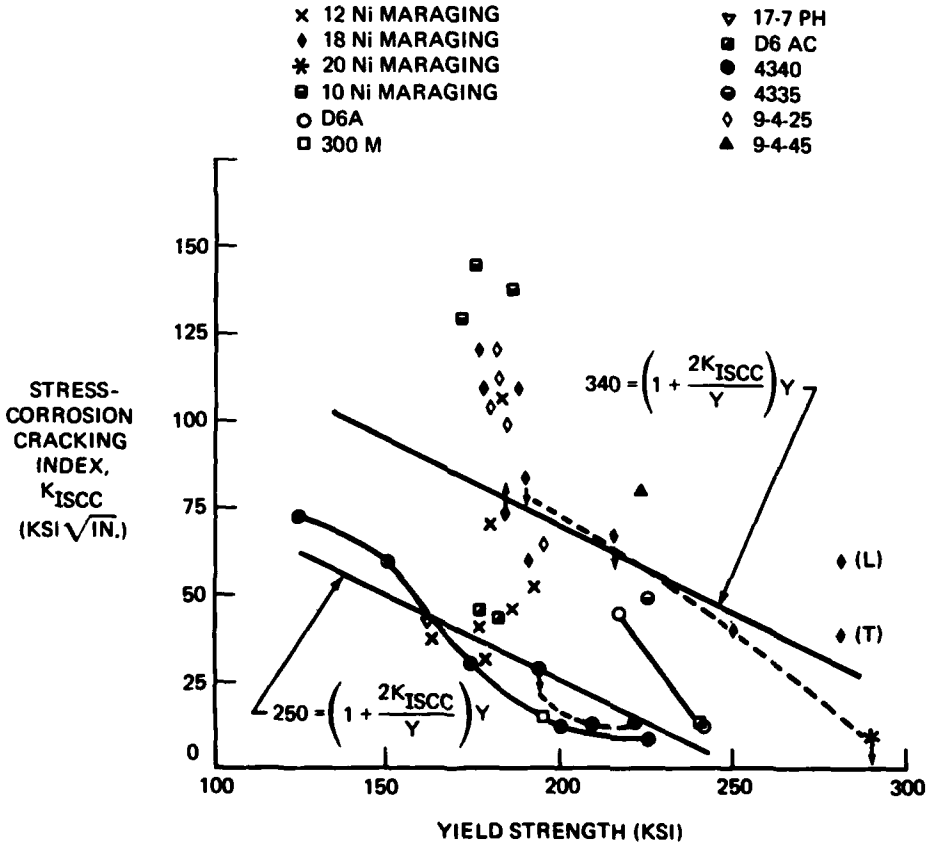

Fig. 21 Summary of K_{ISCC} data (from Ref. 10)

Conclusions

1. Two types of cracking were identified when fatigue precracked notched bend specimens were sustain loaded in 3.5% sodium chloride solution:

   Type 1—a single symmetrical crack extending along the fatigue crack plane.

   Type 2—two divergent cracks extending from the tip of the fatigue precrack.

2. The 300M, H11, Maraging 250, and 9Ni-4Co-0.45C (martensitic) steels exhibited Type 1 cracking. The 4330V, 9Ni-4Co-0.30C, and 9Ni-4Co-0.45C (bainitic) steels exhibited either Type 1 or Type 2 cracking, depending on the K_{Ii} level.

3. Type 2 crack morphology appeared to result from crack extension along the crack-tip plastic zones. The state of stress (plane stress or plane strain) had a significant influence on the morphology of the divergent cracks.

4. Type 2 cracks extended preferentially along the regions of plane stress relaxation. This is contrary to current views which consider that plane stress conditions provide resistance to environmental cracking.

5. Secondary cracks extending from the primary Type 1 crack during propagation through specimens of the 300M and 9Ni-4Co-0.45C (martensitic) steels had a blunting effect. The apparent critical stress-intensity factor to initiate brittle fracture was, in many specimens, about twice the K_{IC} value for a sharp crack.

6. The relationship between K_{ISCC} and yield strength Y was expressed by the empirical relationship $\sigma_{max} = (1 + 2\,K_{ISCC}/Y)\,Y$, where σ_{max} is considered to be the critical normal stress at the precrack tip. Martensitic microstructures containing transformation twins had similar critical normal stress values despite differences in composition and strength level. This stress was significantly higher when transformation twins were absent.

7. This critical stress criterion implies that when the value of K_{ISCC} divided by the yield strength is less than approximately 0.1, the threshold stress intensity for environmental cracking will be independent of thickness.

References

1. B. F. Brown, "A New Stress Corrosion Cracking Test for High-Strength Alloys," Materials Research & Standards, 6, March 1966, p. 129

2. B. F. Brown, "Stress-Corrosion Cracking and Corrosion Fatigue of High-Strength Steels," in "Problems in the Loading-Carrying Application of High-Strength Steels," DMIC Report 210, 1964, p. 91

3. M. H. Peterson, B. F. Brown, R. L. Newbegin, and R. E. Groover, "Stress-Corrosion Cracking of High Strength Steels and Titanium Alloys in Chloride Solutions at Ambient Temperature," Corrosion, 23, 1967, p. 142

4. E. H. Phelps and A. W. Loginow, "Stress Corrosion of Steels for Aircraft and Missiles," Corrosion, 16, 1960, p. 325

5. G. A. Dreyer and W. C. Gallaugher, "Investigation into the Effects of Stress-Corrosion in High Strength Steel Alloys," Air Force Materials Laboratory Report ML-TDR-64-3, 1964

6. G. R. Irwin, "Fracture," Handbuch Der Physik, 6, 1958, Springer, Berlin, p. 551

7. J. L. Guthrie, "High Strength Steel Evaluation for Supersonic Aircraft," Commercial Supersonic Transport Program, Phase IIC Report, Contract FA-SS-66-5, Boeing Document D6A10093-2, March 1967

8. W. F. Brown and J. E. Srawley, "Fracture Toughness Testing," Fracture Toughness Testing and Its Applications, ASTM, STP 381, 1965, p. 133

9. W. A. Van Der Sluys, "Mechanisms of Environment Induced Subcritical Flaw Growth in AISI 4340 Steel," University of Illinois T&AM Report No. 292, 1966

10. G. Sandoz, presentation to ARPA Coupling Meeting on Stress-Corrosion Cracking, held at Carnegie Institute of Technology, June 1967

11. W. D. Benjamin and E. A. Steigerwald, "Stress-Corrosion Cracking Mechanisms in Martensitic High Strength Steels," Air Force Materials Laboratory Technical Report, AFML-TR-67-98, 1967

12. B. F. Brown and C. D. Beacham, "A Study of the Stress Factor in Corrosion Cracking," Corrosion Science, 5, 1965, p. 745

13. J. H. Mulherin, "Stress-Corrosion Susceptibility of High-Strength Steel in Relation to Fracture Toughness," ASME Paper No. 66-Met-5, 1966

14. G. Sandoz and R. L. Newbegin, "Stress-Corrosion Cracking Resistance of an 18Ni 200-Grade Maraging Steel Base Plate and Weld," NRL Memorandum Report No. 1772, 1967

15. C. F. Tiffany and J. N. Masters, "Applied Fracture Mechanics," Fracture Toughness Testing and Its Applications, ASTM, STP 381, 1965, p. 249

16. W. F. Brown and J. E. Srawley, "Plane Strain Crack Toughness Testing of High Strength Metallic Materials," ASTM, STP 410, 1967

17. F. A. McClintock and G. R. Irwin, "Plasticity Aspects of Fracture Mechanics," Fracture Toughness Testing and Its Applications, ASTM, STP 381, 1965, p. 84

18. G. R. Irwin, "Plastic Zone Near a Crack and Fracture Toughness," Proc. Seventh Sagamore Ordnance Materials Research Conference, 1960

19. G. T. Hahn and A. R. Rosenfield, "Sources of Fracture Toughness: The Relation Between K_{IC} and Ordinary Tensile Properties of Metals," presented at ASTM Symposium "Applications Related Phenomena in Titanium and Its Alloys," Los Angeles, 1967

20. J. F. Knott and A. H. Cottrell, "Notch Brittleness in Mild Steel," Journal of the Iron and Steel Institute, 201, 1963, p. 249

21. A. P. Green and B. B. Hundy, "Initial Plastic Yielding in Notch Bend Tests," Journal of Mechanics and Physics of Solids, 4, 1956, p. 128

22. T. R. Wilshaw and P. L. Pratt, "On the Plastic Deformation of Charpy Specimens Prior to General Yield," Journal of Mechanics and Physics of Solids, 14, 1966, p. 7

23. W. W. Gerberich, "Plastic Strains and Energy Density in Cracked Plates," Experimental Mechanics, 4, 1964, p. 335

24. J. E. Truman, R. Perry, and G. N. Chapman, "Stress-Corrosion Cracking of Martensitic Stainless Steels," Journal of the Iron and Steel Institute, 202, 1964, p. 745

25. C. D. Beacham, T. C. Lupton, and J. A. Kies, "The Effects of Three Aqueous Environments on High-Stress Low-Cycle Fatigue," NRL Memorandum Report 1627, 1965

26. A. R. Troiano, "The Role of Hydrogen and Other Interstitials in the Mechanical Behavior of Metals," Trans. ASM, 52, 1960, p. 54

27. A. R. Elsea and F. R. Fletcher, "Hydrogen Induced, Delayed, Brittle Failures of High Strength Steel," DMIC 196, 1964

28. A. S. Tetleman, "The Hydrogen Embrittlement of Ferrous Alloys," in "Fracture of Solids," Wiley, New York, 1963

29. T. Boniszewski, F. Watkinson, R. G. Baker, and H. F. Tremlett, "Hydrogen Embrittlement and Heat-Affected Zone Cracking in Low-Carbon Alloy Steels with Acicular Microstructures," British Welding Journal, 12, 1965, p. 14

30. J. C. Scully and T. P. Hoar, "Morphology of Stress Corrosion Cracks in Notched Specimens of Austenitic Stainless Steels," Corrosion, 20, 1964, p. 174

31. J. E. Truman and R. Perry, "The Resistance to Stress-Corrosion Cracking of Maraging and Other High Strength Steels," Iron and Steel, December 1964

32. R. Hill, "Mathematical Theory of Plasticity," Oxford, London. 1950

33. E. Orowan, "Classical and Dislocation Theories of Brittle Fracture," Fracture, Wiley, New York, 1959, p. 147

34. A. H. Cottrell, "Mechanics of Fracture in Large Structures," Proc. Roy. Soc., Series A, 285, 1965, p. 10

35. G. T. Hahn and A. R. Rosenfield, "Experimental Determination of Plastic Constraint Ahead of a Sharp Crack Under Plane Strain Conditions," Trans. ASM, 59, 1966, p. 909

36. A. S. Tetleman, discussion to the presentation of Reference 35, ASM Annual Meeting, Cleveland, Ohio, 1967

37. J. F. Knott, discussion to "A Discussion on Damage and Failure Mechanisms of Heavy Section Steel," Proc. Roy. Soc., Series A, 285, 1965, p. 150

38. A. J. Baker, F. J. Lauta, and R. P. Wei, "Relationships Between Microstructure and Toughness in Quenched and Tempered Ultra-High-Strength Steels," Structure and Properties of Ultra-High-Strength Steels, ASTM, STP 370, 1965

39. T. Boniszewski, discussion to "Physical Properties of Martensite and Bainite," Iron and Steel Institute Special Report No. 93, 1965

40. B. G. Reisdorf and A. J. Baker, "The Kinetics and Mechanisms of the Strengthening of Maraging Steels," Air Force Materials Laboratory Technical Report M1-TR-64-390, 1964

41. S. R. Novak and S. T. Rolfe, "K_{ISCC} Tests of HY-180/210 Steels and Weld Metals," U.S. Steel Report, Project No. 39.018-007(12), August 1, 1967

42. H. L. Leichter, "Impact Fracture Toughness and Other Properties of Brazed Metallic Laminates," Journal of Spacecraft and Rockets, 3, 1966, p. 1113

Unclassified

Security Classification

DOCUMENT CONTROL DATA - R & D

(Security classification of title, body of abstract and indexing annotation must be entered when the overall report is classified)

1. ORIGINATING ACTIVITY (*Corporate author*)
The Boeing Company
Commercial Airplane Division
Renton, Washington

2a. REPORT SECURITY CLASSIFICATION

2b. GROUP

3. REPORT TITLE

Crack Extension in Several High-Strength Steels Loaded in 3.5% Sodium Chloride Solution

4. DESCRIPTIVE NOTES (*Type of report and inclusive dates*)
Research Report

5. AUTHOR(S) (*First name, middle initial, last name*)
Clive S. Carter

6. REPORT DATE	7a. TOTAL NO. OF PAGES	7b. NO. OF REFS
November 1967	29	42

8a. CONTRACT OR GRANT NO	9a. ORIGINATOR'S REPORT NUMBER(S)
No. N00014-66-C0365	
b. PROJECT NO.	
c.	9b. OTHER REPORT NO(S) (*Any other numbers that may be assigned this report*)
d.	Boeing Document D6-19770

10. DISTRIBUTION STATEMENT
Reproduction in whole or in part is permitted by the United States Government. Distribution of this document is unlimited.

11. SUPPLEMENTARY NOTES	12. SPONSORING MILITARY ACTIVITY
	Advanced Research Projects Agency, Department of Defense

13. ABSTRACT

The morphology of crack growth was determined on precracked, notched bend specimens of 300M, H11, Maraging 250, 4330V, 9Ni-4Co-0.30C, and 9Ni-4Co-0.45C (martensitic and bainitic) steels four-point loaded in 3.5% sodium chloride solution. Crack extension from the tip of the fatigue precrack was either by a single crack that propagated along the fatigue crack plane (Type 1 cracking) or by two divergent cracks that propagated at an angle to the fatigue crack plane (Type 2 cracking). The 4330V, 9Ni-4Co-0.30C, and 9Ni-4Co-0.45C (bainitic) showed either Type 1 or Type 2 cracking, depending on the initial stress-intensity level K_{Ii}. The remaining steels exhibited only Type 1 cracking. The state of stress had a significant effect on the morphology of Type 2 cracks. The morphology suggests that Type 2 cracking is a result of environmental cracking along crack-tip plastic zones. The influence of yield strength on K_{ISCC} can be described by an empirical expression.

DD FORM 1 NOV 65 1473

Unclassified

Security Classification

Unclassified

Security Classification

14. KEY WORDS	LINK A		LINK B		LINK C	
	ROLE	WT	ROLE	WT	ROLE	WT
Stress Corrosion						
High Strength Steels						
Crack Morphology						
Fracture Mechanics						

Unclassified

Security Classification